Primary Research Article

Podocalyxin and ciliary neurotrophic factor receptor are novel components of the surfaceome of chondrogenic cells

Patrik Kovács[1], Peter Brazda[2], Tibor Hajdú[1], Boglárka Harsányi[1], Krisztián Juhász[1], Roland Takács[1], Judit Vágó[1], Zhangzheng Wang[1], Clare Coveney[3], David J. Boocock[3], Csaba Matta[1,*]

[1] *Department of Anatomy, Histology and Embryology, Faculty of Medicine, University of Debrecen, Debrecen, H-4032, Hungary*
[2] *Central for Translational Immunology, University Medical Center Utrecht, Utrecht University, Utrecht, The Netherlands*
[3] *School of Science and Technology, Nottingham Trent University, Nottingham NG11 8NF, United Kingdom*

* To whom correspondence should be addressed. Tel: +36-52-255+567; Email: matta.csaba@med.unideb.hu

Running Head: The Chondroprogenitor Surfaceome

Keywords:

surfaceome; chondrogenesis; cartilage regeneration; glycocapture; proteomics; cartilage; osteoarthritis; PODXL; CNTFR

Abstract

Chondrogenesis, the process driving cartilage formation, is critical for advancing strategies in cartilage repair and mitigating osteoarthritis (OA) management. In this study, we present the first comprehensive quantitative analysis of the surfaceome of chondrogenic cells using a well-established *in vitro* chondrogenic model. By employing sialic acid-targeted glycocapture enrichment of surface proteins coupled with high-throughput shotgun mass spectrometry, we identified podocalyxin (PODXL) and ciliary neurotrophic factor receptor (CNTFR) as novel components of the chondrogenic cell surfaceome. The expression and function of CNTFR and PODXL on chondrogenic cells were validated using western blotting, immunocytochemistry and transient gene silencing. Notably, silencing of CNTFR and PODXL revealed divergent transcriptional effects on COL1A1, a key marker of fibrocartilage and matrix quality, indicating opposing roles in regulating extracellular matrix composition and chondrocyte identity. The identification of PODXL and CNTFR provides new insights into the molecular mechanisms underlying chondrogenesis. The expression of CNTFR on chondrogenic cells suggests a potential role for neurotrophic factors in chondrogenesis and cartilage repair strategies. PODXL, a sialomucin linked to cell-matrix interactions and migration, is potentially involved in maintaining early chondrocyte phenotypes and mediating chondrogenic signals. Altered PODXL and CNTFR in synovial fluid or serum could represent diagnostic biomarkers for early OA, enabling minimally invasive monitoring of cartilage degeneration. Their expression could also be leveraged to monitor disease progression and evaluate therapeutic efficacy. Furthermore, these proteins represent promising targets for OA treatment by modulating their associated signalling pathways to enhance cartilage repair. The detailed profiling of the chondrogenic cell surfaceome establishes a foundation for mechanistically informed biomarkers and pathway-specific therapies to restore cartilage homeostasis in cartilage-related disorders such as OA.

(268 words in Abstract)

Introduction

Osteoarthritis (OA) is the most prevalent form of arthritis, characterized by progressive degeneration of articular cartilage, subchondral bone sclerosis, synovial inflammation, osteophyte formation, and the subsequent deterioration of joint function, resulting in chronic pain and disability (Mobasheri et al., 2023). The global burden of OA is substantial, affecting over 303 million adults globally (Tong et al., 2022) and significantly impairing quality of life. Despite the high prevalence of this degenerative joint disorder, there are currently no FDA-approved disease-modifying osteoarthritis drugs (DMOADs) that can effectively change disease progression or promote cartilage repair. This is partly due to the heterogeneous nature of OA and incomplete understanding of its molecular drivers (Rodriguez-Merchan, 2023). Total joint arthroplasty, while effective short-term, is not an ideal solution for younger patients with OA due to higher risks of prosthesis failure, increased likelihood of revision surgery, unmet functional expectations, and inadequate postoperative pain relief, highlighting the need for alternative management strategies (Bayliss et al., 2017). Existing treatments primarily focus on alleviating symptoms, which underscores an urgent medical need for novel therapeutic strategies in the management of OA (Maqbool et al., 2021).

Cartilage regenerative medicine has emerged as a promising field for addressing this gap. Stem cell-based therapies, particularly those relying on mesenchymal stem cells (MSCs), have attracted interest for their potential to regenerate damaged cartilage and restore joint function (Richardson et al., 2016). However, the clinical efficacy of these approaches has been limited (Muthu et al., 2023). A significant challenge is the poor survival of transplanted MSCs in the inflammatory joint microenvironment and limited integration with native cartilage, which often result in transient benefits without lasting ECM restoration (Tong et al., 2022). Also, stem cell-based regenerative approaches do not lead to substantial structural improvements in the joint, raising concerns about such treatments compared to traditional therapies such as intra-articular corticosteroids and hyaluronic acid (Im and Kim, 2020). Understanding the molecular background of chondrogenesis, including not only lineage progression but also the regulation of extracellular matrix (ECM) composition, is crucial for developing more effective cartilage

tissue engineering strategies. The identification of previously unrecognized biomarkers in chondroprogenitor cells could help tailor specific therapeutic interventions by assessing the efficacy of treatments, and could also enable patient stratification and personalized therapies, addressing OA heterogeneity driven by varied molecular subtypes. This would allow manipulation of the cellular and molecular mechanisms of chondrogenesis, improving cartilage regeneration.

Consequently, the in-depth profiling of the surfaceome; i.e., the dynamic complement of cell surface proteins, has become critical in understanding the biology of chondroprogenitor cells and their potential to optimise cartilage tissue engineering (Matta et al., 2019a; Pauwels et al., 2022; Takacs et al., 2025). The surfaceome plays a crucial role in mediating cell-matrix interactions, signalling pathways, responses to the extracellular environment, and in regulating ECM remodelling during chondrogenic differentiation. Currently, the surfaceome of chondrogenic cells is incompletely understood. Several currently accepted surface markers (e.g., CD44, CD73) show inconsistent correlation with the chondrogenic potential of MSCs derived from different tissues (Alegre-Aguaron et al., 2012), which calls for the development of novel techniques to discover more reliable surface markers to meet the demands of regenerative medicine (Lu et al., 2020). By profiling the surfaceome of chondrogenic cells, we will be better placed to identify novel biomarkers that may enhance the efficacy of regenerative therapies. Such biomarkers could facilitate the selection of optimal cell types for therapy, enhance the engraftment and survival of administered cells, and guide biomaterial design to mimic native chondrogenic niches (Kalamegam et al., 2018).

This study provides a temporal landscape of the surfaceome of chicken embryonic limb bud-derived chondrogenic progenitor cells spontaneously undergoing chondrogenesis in micromass cultures. We conducted a comprehensive quantitative proteomics analysis of chondrogenic cell cultures at key stages of chondrogenesis. Utilizing high-throughput shotgun liquid chromatography-tandem mass spectrometry (LC-MS/MS), we analysed total cell lysates to identify proteins associated with the differentiation process. Furthermore, we enriched the cell surface subproteome through a sialoglycoprotein-specific glycocapture technique using

aminooxy-biotin, followed by shotgun proteomics (Matta et al., 2019a; Jeremiasse et al., 2020; Kovacs et al., 2025). This approach allowed us to delineate the surfaceome of chondrogenic cells and uncover proteins that have not previously been implicated in chondrogenic differentiation. Notably, we identified podocalyxin (PODXL), a sialomucin regulating renal podocyte polarity, and ciliary neurotrophic factor receptor (CNTFR), a neurotrophic signal transducer, as previously unknown constituents of the chondrogenic surfaceome. Their chondrogenic expression suggests co-operation between adhesion and survival mechanisms, offering exciting new targets for research and potential therapeutic applications in cartilage regeneration.

Materials and Methods

1. Experimental setup

This study employed a staged approach to define the surfaceome of embryonic chicken limb bud-derived chondrogenic cells at key stages of chondrogenic differentiation. Temporal proteomic profiling was conducted at days 1, 3, 6, 10, and 15 of micromass culture, combining sialoglycoprotein enrichment via aminooxy-biotin conjugation with high-resolution LC-MS/MS. After proteins quantification, GO term enrichment analysis was carried out to prioritize chondrogenesis-associated pathways. Candidate surface markers ciliary neurotrophic factor receptor (CNTFR) and podocalyxin (PODXL) were validated through RT-qPCR, western blotting, and immunocytochemical localization. The integrated workflow, spanning discovery to functional validation, is summarized in Figure 1.

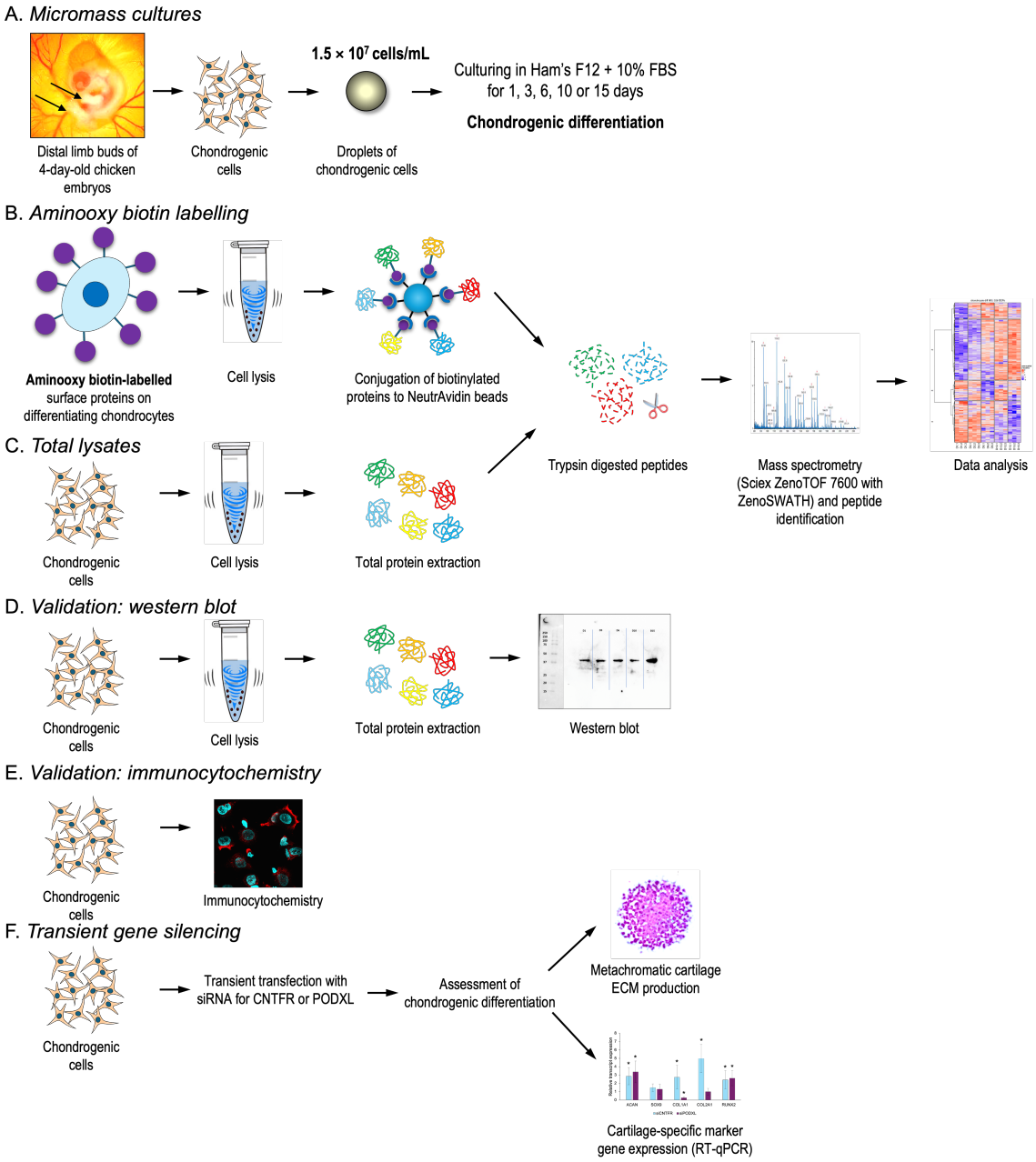

Figure 1. Experimental workflow.

2. Chondrogenic micromass cultures

Chondrogenic micromass cultures were established from embryonic chicken limb bud chondroprogenitor using a standardized protocol optimized for spontaneous chondrogenesis (Takacs et al., 2023a). Briefly, distal parts of limb buds were carefully excised from early-stage (4.5 days old); Hamburger–Hamilton 22–24) chicken embryos. The isolated and pooled limb buds were dissociated into a single-cell suspension via trypsin-EDTA digestion. Cells were

resuspended in Ham's F12 medium (Gibco, Thermo Fisher Scientific, Waltham, MA, USA) supplemented with 10% foetal bovine serum (FBS, Gibco) and plated as 100 µL micromass droplets (1.5×10^7 cells/mL) onto 6-well plates. Following a 2-hour adhesion phase (37°C, 5% CO_2), cultures were gently flooded with fresh medium to maintain 3D architecture. Chondrogenesis proceeds spontaneously in this culture system, as evidenced by the appearance of cartilaginous nodules and an abundant cartilage-specific ECM. This model recapitulates *in vivo* chondrogenesis, including COL2A1 upregulation and SOX9-dependent ECM synthesis, as previously characterized in this system (Takacs et al., 2023a; Takacs et al., 2023b). Cultures were harvested at days 1, 3, 6, 10, and 15 to capture key transitions in surfaceome dynamics during early differentiation.

3. Sample preparation for LC-MS/MS: Cell surface proteome labelling and enrichment, and total cell lysates

For a detailed methodology for cell surface sialoglycoprotein labelling and enrichment of chondroprogenitor cells in micromass cultures, please see our protocol paper (Kovacs et al., 2025). Unless otherwise stated, all reagents were purchased from Thermo Fisher Scientific. Briefly, sialic acid residues on the cell surface proteins of micromass cultures on culture day 1, 3, 6, 10, and 15 were oxidized using 1 mM sodium meta-periodate to generate reactive aldehyde groups. This was followed by incubation in the dark for 1 hour at 4°C with 100 mM aminooxy-biotin (Biotium, Fremont, CA, USA), with gentle rocking to ensure uniform labelling. After quenching with glycerol, the labelled cells were lysed (1% Triton X-100, 150 mM NaCl, 5 mM iodoacetamide, 10 µL protease inhibitor cocktail, 0.1 mg/mL PMSF and 10 mM Tris-HCl; pH 7.6). Biotinylated proteins were affinity-purified using NeutrAvidin agarose beads, allowing for the selective capture of labelled surface proteins. This was followed by stringent washes including lysis buffer and 0.5% (w/v) SDS in PBS to remove nonspecific binders. Captured protein were reduced by 100 mM DTT and alkylated in 50 mM iodoacetamide, further wash steps were performed with UC buffer (6 M urea, 100 mM Tris-HCl; pH adjusted to 8.5), 5M NaCl, 100 mM Na_2CO_3, PBS (pH 7.4), and HPLC grade water to

minimize contamination from intracellular components, and to prepare the sample for LC-MS/MS analysis. Captured proteins were digested overnight with 5 µg MS-grade trypsin in 50 mM NH_4HCO_3. Solvents were then evaporated in a vacuum concentrator centrifuge and stored at –80°C until analysis.

Parallel total proteome analysis of micromass cultures harvested on the same culture days as above were prepared using lysis in RIPA and sonication to shear DNA (3 × 10 sec pulses), ensuring membrane protein solubilization. Samples were then stored at –80°C until analysis. This dual approach enabled comparative quantification of surface-enriched vs. intracellular proteins during chondrogenesis.

4. Mass spectrometry, protein identification and quantification

Dried peptide samples were reconstituted in 150 µL of 10% acetonitrile with 0.1% formic acid, shaken at 5°C for 20 minutes, followed by addition of 150 µL 0.1% formic acid to yield a final concentration of 5% acetonitrile and 0.1% formic acid. After centrifugation at 12,000 × g for 2 minutes to remove particulates, supernatants were transferred to LC-MS compatible vials. Peptide separation was performed on a Waters M-Class UPLC system equipped with a Phenomenex Kinetex XB-C18 column (2.6 µm, 15 × 0.3 mm) maintained at 30°C, using a linear gradient of 3–35% acetonitrile (mobile phase B) over 12 minutes at a flow rate of 10 µL/min, followed by washing at 80% B and re-equilibration to 3% B. Three microlitres of each sample were injected in direct inject mode. Mass spectrometric analysis was conducted on a Sciex 7600 ZenoTOF operating in positive ion mode with Data Independent Acquisition (DIA, zenoSWATH), employing a 25 ms TOF-MS scan and 65 variable SWATH windows (12 ms each) covering m/z 400–750, with a total cycle time of 1.146 s. Raw data files (.wiff, .wiff2, .wiff.scan) were processed using DIA-NN (version 1.8.1) (Demichev et al., 2020), with a *Gallus gallus* UniProt FASTA database (downloaded Oct 2021), enabling library-free search and deep learning-based spectra prediction. Label-free quantification was performed at a precursor FDR of 1.0%, with default DIA-NN parameters unless otherwise specified. Protein identification and quantification results were exported as .tsv files, and proteins were

annotated using Gene Ontology (GO) information from UniProt to infer cell surface/plasma membrane localization.

The mass spectrometry proteomics data have been deposited to the ProteomeXchange Consortium *via* the PRIDE partner repository with the dataset identifier PXD064013.

5. Protein and gene expression analysis using bioinformatics, pathway analysis

Proteomic intensity data were log2-transformed. Missing values were imputed using a left-censored normal distribution via the minProb method (q = 0.001) from the *promor* package in R (Ranathunge et al., 2023) to simulate low-abundance signals below the detection threshold. Entries representing protein families (where individual proteins could not be reliably deconvoluted) were excluded from the downstream bioinformatic analysis workflow, as some of these were also present as single entries in the matrix. Principal component analysis (PCA) was used to assess sample variability and potential batch effects.

Differential protein expression (DEP) analysis was performed using the *DEqMS* package in R, applying linear modeling with variance moderation based on peptide counts. Proteins with |log2 fold-change| > 1 and Benjamini-Hochberg adjusted p-value < 0.05 were considered DEPs. The *gorth* package was used to perform ortholog mapping from chicken (*Gallus gallus*) to human (*Homo sapiens*). The resulting set of DEPs was z-score scaled and grouped using hierarchical clustering to identify temporal expression patterns.

Gene Ontology (GO) enrichment analysis was performed for each DEP analysis and temporal DEP cluster using enrichGO() and compareCluster() (*org.Hs.eg.db*, p-value < 0.05, q-value < 0.2), covering Biological Process (BP), Molecular Function (MF), and Cellular Component (CC) categories. Statistical analysis and visualization were carried out in R.

Cell surface/plasma membrane ("surfaceome") proteins were inferred according to the protein annotation and Gene Ontology (GO) information downloaded from the UniProt database (www.uniprot.org). We used a combination of the following GO terms (cellular component, biological process) to infer plasma membrane localisation to maximise the

discovery of cell surface proteins (Kovacs et al., 2025): [GO:0016020] membrane; [GO:0031012] extracellular matrix; [GO:0005576] extracellular region; [GO:0005615] extracellular space; [GO:0005886] plasma membrane; [GO:0009897] external side of plasma membrane; [GO:0031234] extrinsic component of cytoplasmic side of plasma membrane; [GO:0045121] membrane raft; [GO:0009986] cell surface; [GO:0005890] sodium:potassium-exchanging ATPase complex; [GO:0016324] apical plasma membrane; [GO:0016323] basolateral plasma membrane; [GO:0016328] lateral plasma membrane; [GO:0005905] clathrin-coated pit; and [GO:0060170] ciliary membrane. Some proteins were challenging to categorize into a given cellular compartment, because accurate predictions were limited and experimental evidence lacking. Also, many proteins may be present in multiple cellular compartments. When proteins were found to be annotated in one of the above GO categories referring to the cell surface, this localisation was considered the most likely, since selective surfaceome protein extraction was attempted in this study.

Our previously published NGS dataset (BioProject IDs: PRJNA817177; PRJNA938813) (Takacs et al., 2023b) was processed using R. Weighted gene correlation network analysis (WGCNA) was performed with the WGCNA R package. For the construction of the protein-protein interaction (PPI) network, we utilized the STRING database (https://string-db.org/), and Cytoscape was employed to further screen the proximal associated proteins. Finally, enrichment analysis was carried out using the clusterProfiler R package.

7. Immunocytochemistry

Micromass cultures were established on coverslips as described previously (Matta et al., 2019b). On specified culture days, cells were dissociated using mild collagenase type I treatment (Sigma, St. Louis, MO, USA) for 30 minutes at 37°C, resuspended in fresh F12 medium, and seeded onto glass coverslips in 24-well plates. Cells were allowed to adhere for 2 hours in a humidified incubator (37°C, 5% CO_2). Following attachment, cells were fixed in 10% formalin in 1 × PBS for 30 minutes at room temperature. After washing in PBS, non-

specific binding sites were blocked with 3% bovine serum albumin (BSA, Amresco LLC, Solon, OH, USA) and 10% serum from the host species of the secondary antibody (see below) in PBS for 1 hour at room temperature.

For immunostaining, cells were incubated overnight at 4°C with anti-CNTFR (Abcam, Cambridge, UK; Cat. No. ab127425) at a dilution of 1:500, and anti-PODXL (Proteintech, Manchester, UK; Cat. No. 18150-1-AP) antibodies at a dilution of 1:500, diluted in blocking solution. Primary antibodies were detected using a goat anti-rabbit IgG secondary antibody conjugated to Alexa Fluor 555 (Life Technologies Corporation, Carlsbad, CA, USA; Cat. No. A27039) at a dilution of 1:1000, incubated for 1 hour at room temperature. Cultures were mounted in Vectashield Hard Set mounting medium (Vector Laboratories Ltd., UK) containing DAPI to visualise nuclei. Subcellular localization of PODXL and CNTFR was analysed using an Olympus FV1000S confocal microscope (Olympus Co. Tokyo, Japan) equipped with a 60× oil immersion objective (NA: 1.3). For excitation of AlexaFluor 555, 543 nm laser line was used. The average pixel dwell time was 4 μs. Images of Alexa Fluor 555 and DAPI were overlaid.

8. Western blot analysis

Total cell lysates for SDS–PAGE were prepared as previously described (Matta et al., 2019b). To ensure equal protein loading, after protein concentrations were determined, four-fold concentrated Laemmli buffer (Thermo Fisher Scientific) was added to the lysates, and samples were heated at 95°C for 10 minutes. In each lane, 20 μg of protein per sample was loaded onto 10% SDS–polyacrylamide gels for separation. Following electrophoresis, proteins were transferred onto nitrocellulose membranes using electroblotting. Membranes were blocked with 5% non-fat dry milk dissolved in PBS for 1 hour at room temperature. Subsequently, membranes incubated overnight at 4°C with the primary antibodies (anti-CNTFR at a dilution of 1:500, and anti-PODXL at a dilution of 1:500). After three washes in PBST (PBS containing 0.1% Tween-20) for a total of 30 minutes, membranes were incubated with an anti-rabbit IgG secondary antibody (Bio-Rad Laboratories, CA, USA) in 1:1000 dilution

for 1 hour at room temperature. Protein bands were visualised using enhanced chemiluminescence (Millipore, Billerica, MA, USA) according to the instructions provided by the manufacturer. Equal protein loading was verified by probing for β-actin as a loading control.

9. Transient gene silencing of CNTFR and PODXL

To investigate the impact of transient gene silencing of *CNTFR* and *PODXL* on chondrogenic differentiation, freshly isolated limb bud-derived progenitor cells were transfected with siRNA. Cells were resuspended at a density of 1.5×10^7 cells/mL in 37°C Ham's F12 medium, and seeded into 12-well plates (Catalog no. 92412, Techno Plastic Products). Custom-designed siRNAs targeting CNTFR (Silencer™ Custom Designed siRNA; Cat. no. 4399666, Design ID: ABD1VPK) and PODXL (Silencer™ Custom Designed siRNA; Cat. no. 4399666, Design ID: ABHSP78), along with a non-targeting (NT) control (Silencer™ Select Negative Control No. 1 siRNA; Cat. no. 4390844; Life Technologies, Thermo Fisher Scientific), were transfected into chondrogenic cells 2 hours post-attachment using Lipofectamine™ RNAiMAX Transfection Reagent (Cat. no. 13778150; Life Technologies) and Opti-MEM™ Reduced Serum Medium (Cat. no. 51985034; Life Technologies).

For the analysis of cartilage ECM production following gene silencing, colonies were fixed on culture day 6, stained with DMMB (pH 1.8), and photographed. Cartilage ECM production was quantified using a MATLAB script (Takacs et al., 2023a), with values normalised to NT control levels. Relative cell numbers or viability (inferred from mitochondrial activity) were analysed via MTT assay (Takacs et al., 2023a). Briefly, MTT reagent (5 mg/1 mL PBS) was added to the cells in 24-well plates on culture day 6, incubated for 2 h at 37°C, and solubilized with MTT solubilizing solution. Absorbance was measured at 570 nm (Chameleon, Hidex, Turku, Finland). Optical density values were expressed as percentage changes relative to NT control.

Gene expression profiling of chondrogenic marker genes was performed as described previously (Takacs et al., 2023b) with the following minor adjustments. Micromass cultures were harvested 48 hours post-transfection. Total RNA was isolated using TRI Reagent

(Applied Biosystems) following to the manufacturer's instructions. Total RNA (1 µg) was reverse-transcribed into cDNA using the High-Capacity cDNA Reverse Transcription Kit (Thermo Fisher Scientific) according to the manufacturer's protocol. The expression patterns of chondrogenic marker genes were quantified via CYBR Green-based RT-qPCR using the $2^{-\Delta\Delta Ct}$ method. Primer sequences (Integrated DNA Technologies (Coralville, IA, USA) are provided in Table S1 in Supplementary file 1. RT-qPCR reactions were set up using GoTaq qPCR Master Mix (Promega) and 20 ng of input cDNA per each 10-µL reaction. Reactions were run on a QuantStudio 3 Real-Time PCR System (Thermo Fisher Scientific) using a standard thermal profile (Takacs et al., 2023b). Amplification data were analysed using the QuantStudio Design and Analysis Software (version 1.5.1), and exported for processing in Microsoft Excel (version 2108). Six reference genes were evaluated for stability: hypoxanthine phosphoribosyltransferase 1 (*HPRT1*), peptidylprolyl isomerase A (*PPIA*), ribosomal protein L4 (*RPL4*), 60S ribosomal protein L13 (*RPL13*), ribosomal protein S7 (*RPS7*), and tyrosine 3-monooxygenase/tryptophan 5-monooxygenase activation protein zeta (*YWHAZ*). BestKeeper (Pfaffl et al., 2004), an Excel-based tool, identified *RPS7* as the most stable reference gene through pairwise correlation analysis. All target gene data were normalised to *RPS7* expression.

Results

1. Temporal proteome dynamics in chondrogenic micromass cultures

High-throughput LC-MS/MS analysis was performed on total lysates from chondrogenic micromass cultures harvested at culture days 1, 3, 6, 10 and 15 (N=3 biological replicates), corresponding to key histodifferentiation stges (Takacs et al., 2023a; Takacs et al., 2023b). Across time points, a total of 5,207 proteins/protein groups identified (FDR < 0.05).

Principal component analysis (PCA) revealed distinct proteomic profiles at each differentiation stage, with biological replicates clustering tightly by culture day (Figure 2A–B). The first principal component (PC1), which explains 42% of the variance, captured temporal

progression, separating undifferentiated (day 1) from differentiated (days 10 and 15) cultures. PC2 (19% variance) distinguished intermediate differentiation stages (days 3–6) from both early and late time points.

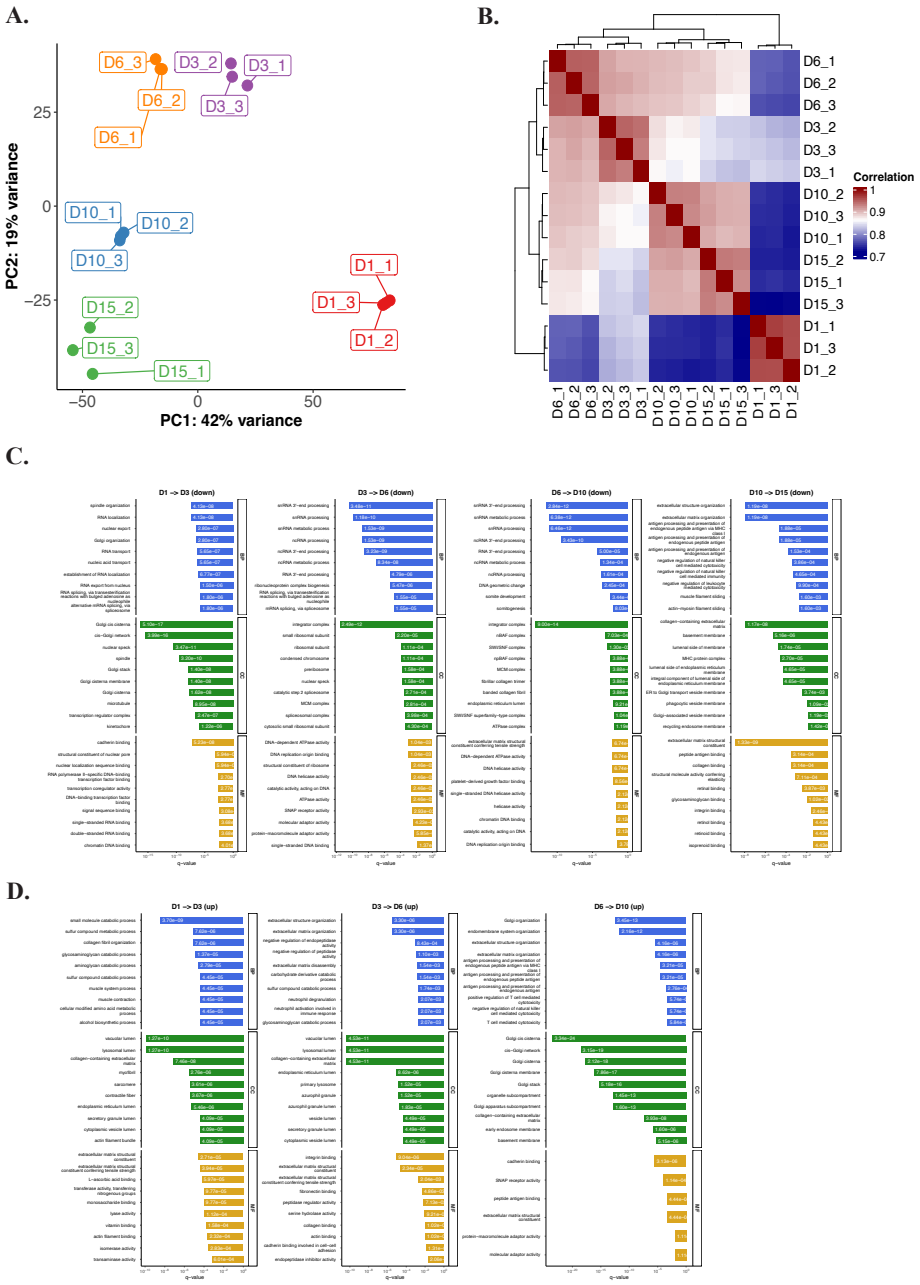

Figure 2. Quantitative proteomics analysis of total cell lysates from chondrogenic micromass cultures. A. Principal component analysis (PCA) of the total lysate samples of micromass cultures of chondroprogenitor cells undergoing chondrogenesis (5,207 proteins in the entire dataset). Each dot represents a biological replicate (N=3). The PCA plot shows unsupervised clustering according to culture age along the principal component (PC) 1 and PC2 hyperplanes, accounting for 42% and 19% of the variance, respectively. **B.** The correlation matrix also demonstrates clear separation among the samples according to culture age. **C–D.** Enrichment analysis using gene ontology (GO) annotations for pairwise comparisons of culture days, showing the top GO terms (biological process (BP), cellular compartment (CC), or molecular function (MF)) by ranking them by the adjusted p-values (p.adjust < 0.001). Plots shown separately for upregulated (**C**, top panel) and downregulated (**D**, bottom panel) proteins. The *x*-axis is the adjusted p-value of the enriched terms.

Using a log2 fold change (|log2FC|) threshold of 1.0, and a Benjamini-Hochberg adjusted p-value (FDR) of less than 0.05, a total of 792 proteins (323, 159, 272, and 38 for each consecutive timepoint comparison: day 1–3, day 3–6, day 6–10, and day 10–15, respectively) were identified as significantly upregulated. Similarly, 1368 proteins (714, 231, 178, and 245 for each corresponding timepoint comparison) were identified as significantly downregulated (Figure S1 in Supplementary file 1). Full lists of differentially expressed proteins (DEPs) for pairwise comparisons between consecutive days and between undifferentiated (day 1) versus mature (day 15) cultures are provided in the Supporting Information (Supplementary file 2).

To better characterise DEPs between each time point, we performed gene ontology (GO) analysis on the DEPs (Figure 2C–D). In case of proteins that were upregulated in consecutive time points, GO terms related to collagen-containing ECM synthesis, ECM organization, and integrin binding were over-represented. In contrast, when we looked at the downregulated DEPs separately, a much broader range of GO terms were identified, such as those related to DNA and RNA metabolism, DNA replication, and transcription factor binding, especially in the earlier time points. Between day 10–15, ECM-related GO terms were also enriched, indicating that ECM production has been completed by day 15 (mature/hypertrophic) cultures.

The identified DEPs in the total lysates of chondrogenic cultures were categorized into 5 clusters to delineate expression dynamics (Figure 3A–B). Protein lists for each cluster are provided in the Supporting Information (Supplementary file 3).

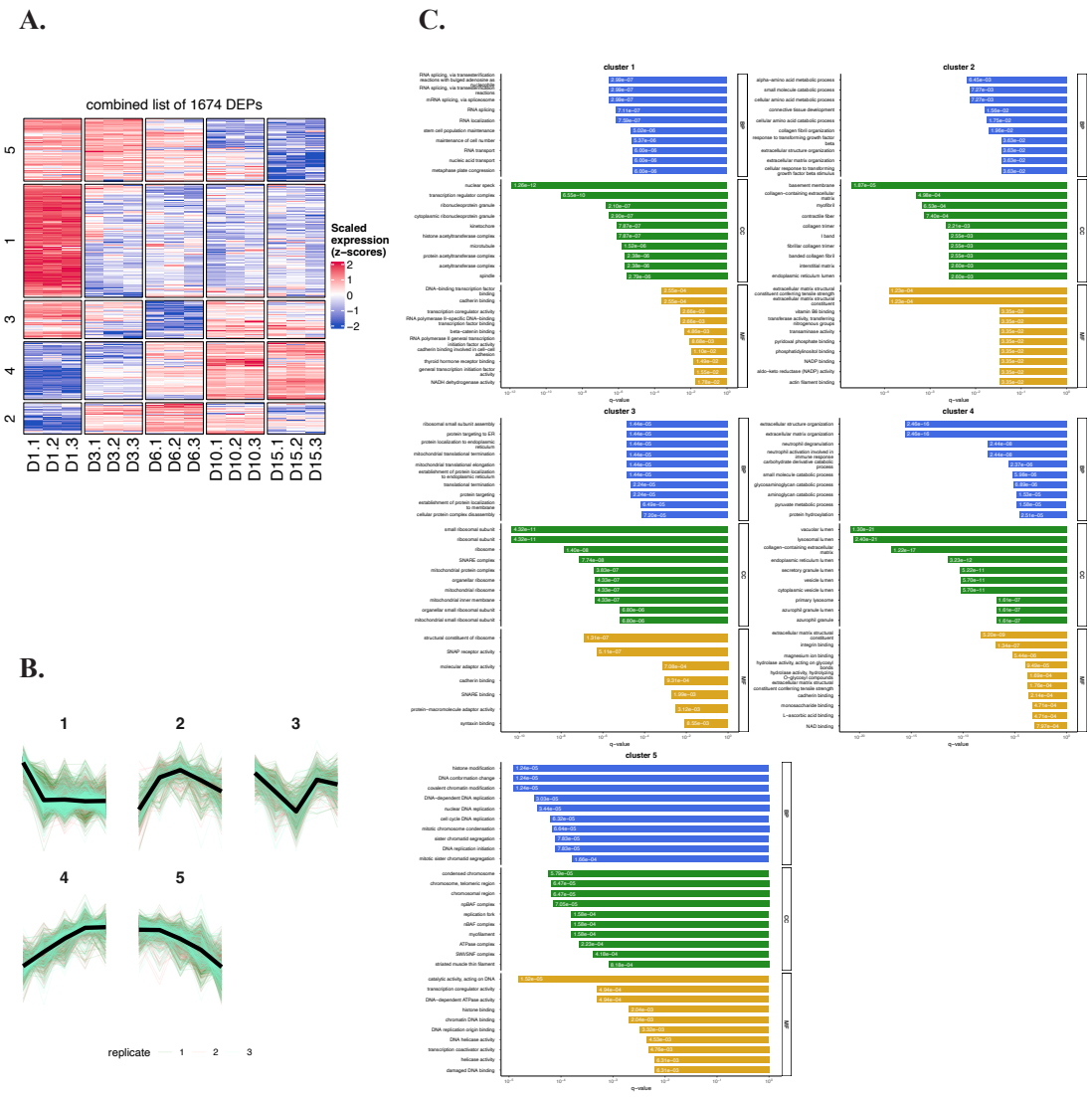

Figure 3. Unsupervised clustering analysis of differentially expressed proteins (DEPs) in total cell lysates of chondrogenic cultures using the k-means algorithm. A–B. The expression dynamics of each cluster are shown in clusters 1–5. *x*-axis, time points (days of culturing). **C.** Pathway analysis using Gene Ontology (GO) annotation for the 5 clusters of proteins in total lysates of chondrogenic cells undergoing chondrogenic differentiation. Select terms for GO biological process (BP), cellular component (CC), and molecular functions (MF). Barplot shows significant terms, the *x*-axis is gene (protein) ratio and the number of proteins belonging to given enriched terms.

Cluster 1 (625 proteins) exhibited an initial steep downregulation during early *in vitro* chondrogenesis (days 1–3), plateauing thereafter. This group of proteins showed enrichment for GO terms related to RNA splicing, histone acetyltransferase activity, and RNA polymerase II mediated transcription (Figure 3C), suggesting phased suppression of transcriptional machinery in maturing cultures. **Cluster 2** (173 proteins) displayed peak expression at day 6, with overrepresented GO terms linked to amino acid metabolism, connective tissue

development, and collagen synthesis. **Cluster 3** (211 proteins) followed a U-shaped trajectory: downregulated initially but upregulated in later stages, and was enriched for GO terms related to mitochondrial functions and ribosomeal function. **Cluster 4** (319 proteins) demonstrated progressive upregulation, peaking in mature chondrocytes (days 10–15), suggesting that these proteins are associated with the later stages of chondrogenic differentiation and may contribute to the functional maturation of chondrocytes. Over-represented GO terms in this cluster were related to ECM and collagen synthesis. **Cluster 5** (346 proteins) showed a similar expression pattern to cluster 1 but with a more sustained downregulation throughout chondrogenesis. Over-represented GO terms in this cluster included histone modification and cell proliferation (DNA replication and chromosome condensation).

Proteins in **Clusters 2 and 4**, which were termed the 'chondrogenic subset' of proteins, contained proteins such as collagens (COL1A1, COL2A1, COL6A1), integrins (ITGA4), matrilin-1 (MATN1), bone morphogenic protein (BMP1), and transforming growth factor receptor beta (TGFB2).

Next, we carried out a detailed protein-protein interaction (PPI) analysis of each cluster using STRING and generated a small network with the top 20 hub proteins (Figure S2 in Supplementary file 1). In the PPI network of **Cluster 1**, spliceosome (SRSF1, DDX5, HNRNPM) and ribosome biogenesis (NOP58, FTSJ3, GNL3) are recurrent pathways. Components of the PI3K–Akt (Akt1) and Wnt (CTNNB1) signalling were also enriched, whereas BIRC5 and SUMO1 regulate apoptosis and post-translational modifications, respectively. The PPI network in **Cluster 2** is centrally enriched in ECM dynamics and cell–matrix signalling (COL1A1, COL5A1, COL5A2, COL12A1, FBN1, THBS2), with focal adhesion (THBS2) and PI3K–Akt (P4HA3) as hub pathways. The proteins in the network of **Cluster 3** are predominantly associated with ribosomal biogenesis (RPS20, RPS14, RPS19, RPS26, RPL13), translation, and RNA processing (NCBP2, SNRPA1), with strong enrichment in conserved pathways such as global protein synthesis, protein processing in endoplasmic reticulum (SEC61B), and mitochondrial translation (MRPS14, MRPS7, MRPL17). In a similar way to Cluster 2, the PPI network of **Cluster 4** is enriched in ECM remodelling, glycolysis, and

cell adhesion signalling. ECM dynamics dominate this cluster, with collagens (e.g., COL6A1, COL2A1) and modifiers (P4HA1/2) driving ECM integrity. Glycolysis enzymes (LDHA, GAPDH) highlight metabolic reprogramming, and focal adhesion and PI3K–Akt couple signalling to pro-survival pathways. For **Cluster 5**, the PPI network is enriched in cell cycle regulation (CDK1, CDK2, AURKB, CDC45, MCM3/4/5, SMC4), DNA replication/repair (MCM3/4/5, CDC45, RFC4, TP53BP1), and chromatin remodelling (CREBBP, EP300, SMARCA4, EZH2).

2. Chondrogenic surfaceome dynamics via aminooxy-biotin enrichment

Following conversion of sialic acid residues into aldehydes, chondrogenic cells were labelled with aminooxy-biotin (AOB) to profile surfaceome changes during differentiation. Enriched biotin-labelled proteins from three biological repeats (N=3) underwent high-throughput LC-MS/MS analysis at the same time points as total lysates (days 1, 3, 6, 10, and 15). Of 522 quantified proteins/protein groups, 18 detected in only one time point were excluded, leaving 504 proteins for differential protein expression analysis. PCA revealed low degree of variability among biological replicates, with clear separation by culture day along PC1 (40% variance) (Figure 4). This trajectory mirrored trends observed in the total proteome, reflecting stage-specific surfaceome dynamics as cells progressed from undifferentiated (day 1) to mature (day 15) states.

Based on a log2 fold change (|log2FC|) threshold of 1.0 and a Benjamini-Hochberg adjusted p-value (FDR) of less than 0.05, a total of 254 proteins (72, 74, 89, and 19 for each consecutive timepoint comparison: day 1–3, day 3–6, day 6–10, and day 10–15, respectively) were identified as significantly upregulated. Similarly, 170 proteins (10, 82, 31, and 47 for each corresponding timepoint comparison) were identified as significantly downregulated (Figure S3 in Supplementary file 1). DEP lists for pairwise comparisons of subsequent culture days are provided in the Supporting Information (Supplementary file 4).

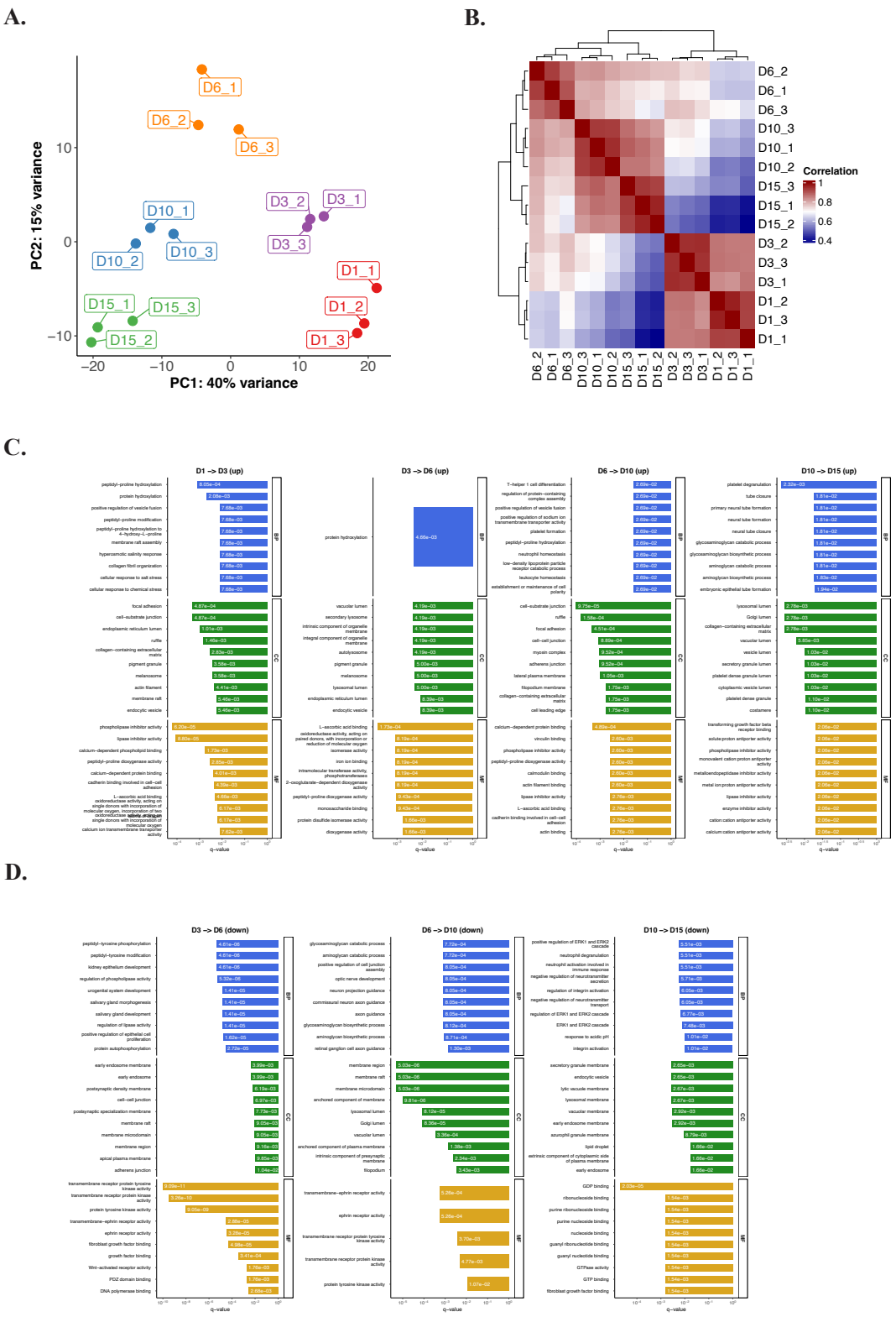

Figure 4. Quantitative proteomics analysis of aminooxy biotin (AOB) enriched samples from chondrogenic micromass cultures. A. PCA of the AOB-enriched samples of micromass cultures undergoing chondrogenesis (504 proteins in the dataset). Each dot represents a biological replicate (N=3). The samples clustered together according to culture age along the principal component (PC) 1 and PC2 hyperplanes, which account for 40% and 15% of the variance, respectively. **B.** The correlation matrix (right panel) also signifies separation among the samples according to differentiation status. **C–D.** Pathway analysis using Gene Ontology

(GO) annotation for the AOB-enriched subproteome of chondrogenic cells undergoing chondrogenic differentiation. Panel shows the top GO terms based on biological process (BP), cellular compartment (CC), or molecular function (MF), separately for upregulated (**C**, top panel) and downregulated (**D**, bottom panel) proteins, following ranking by adjusted p-values. The *x*-axis is the adjusted p-value of the enriched terms.

We performed GO analysis on DEPs that were up or downregulated in later time points using g:profiler to better characterise DEPs between each time point (Figure 4C–D). Upregulated proteins were enriched in collagen biosynthesis (terms such as peptidyl-prolyl hydroxylation, L-ascorbic acid binding), ECM maturation (glycosaminoglycan biosynthesis), and cell-matrix adhesion, consistent with chondrocyte functional specialisation. In contrast, GO terms associated with downregulated DEPs included developmental signalling (ephrin receptor pathway, Wnt-activated receptor activity, regulation of ERK1 and ERK2 cascade), growth factor modulation, and several terms related to neural processes (synapses and axonal growth), suggesting attenuation of plasticity pathways in mature cells.

Proteins in the aminooxy-biotin-enriched subproteome were classified into four clusters based on expression dynamics (Figure 5A–B). Protein lists for each cluster are provided in the Supporting Information (Supplementary file 5).

Cluster 1 (96 proteins) exhibited progressive upregulation during *in vitro* chondrogenesis, enriched in GO terms such as ECM organization, L-ascorbic acid binding, and peptidyl-prolyl hydroxylation (related to collagen alpha-chain synthesis), and bone development (Figure 5C). **Cluster 2** (60 proteins) showed peak expression on culture day 6, with overrepresented GO terms such as kinase activity, ephrin receptor activity, growth factor binding, and FGF signalling. **Cluster 3** (63 proteins) displayed transient suppression on culture day 6, followed by late-stage upregulation in mature cultures, with overrepresented GO terms related to RNA polymerase II and the cell cycle. **Cluster 4** (88 proteins) declined steadily after day 3 in mature chondrocytes, suggesting roles restricted to early differentiation. Enriched GO terms in this cluster include muscle and nervous system development, as well as tyrosine kinase and growth factor signalling.

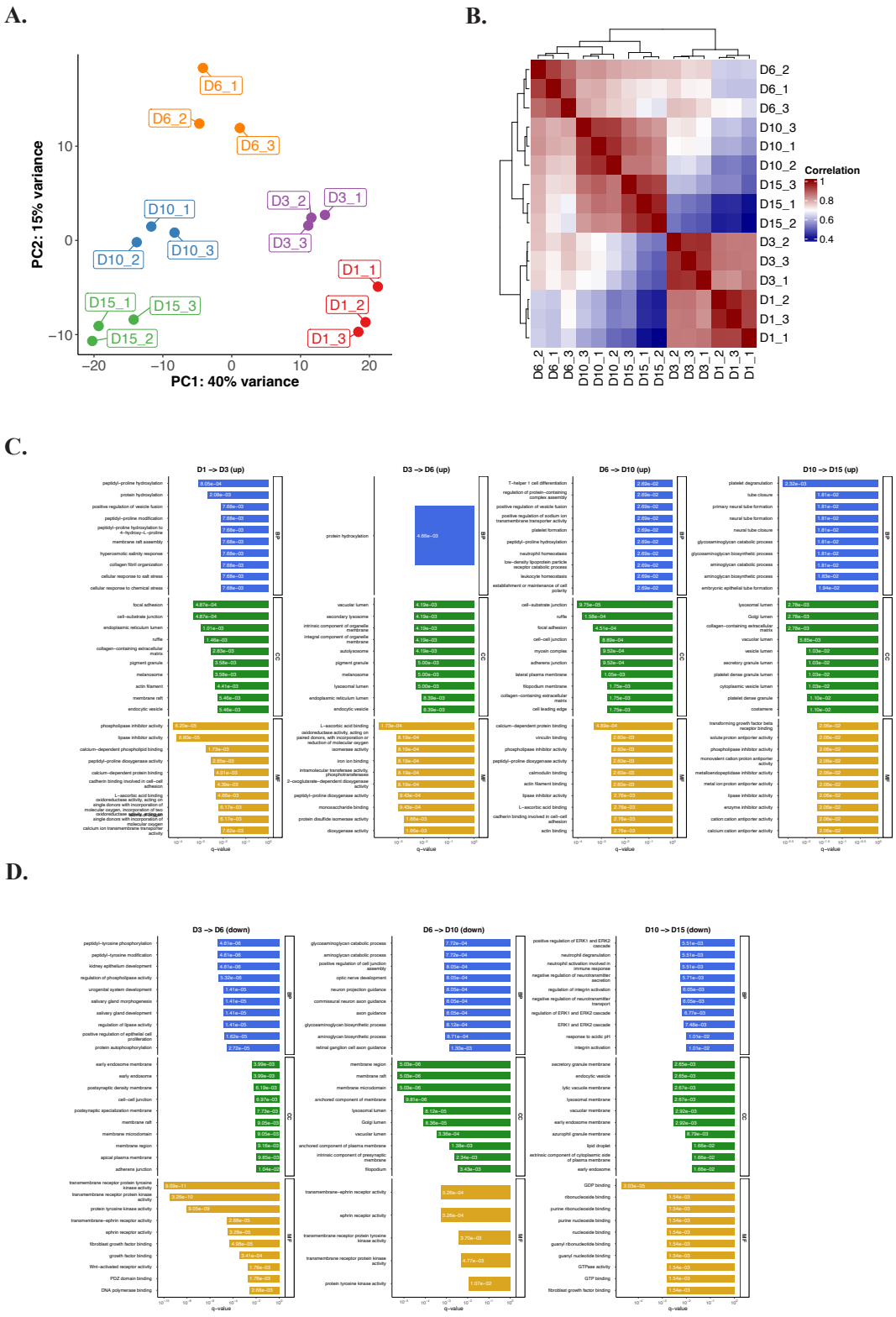

Figure 5. Unsupervised clustering analysis of differentially expressed proteins in the AOB-enriched subproteome during chondrogenesis using the k-means algorithm. A–B. The expression dynamics of each cluster are visible in clusters 1–4. The *x*-axis represents the time points (days of culturing). **C.** Pathway analysis using Gene Ontology (GO) annotation for the 4 clusters. Selected terms for GO biological processes (BP), cellular component (CC), and molecular functions (MF). Barplot shows significant terms, the *x*-axis is gene (protein) ratio and the number of proteins belonging to given enriched terms.

Clusters 1 and 3 contained those proteins whose surface expression was associated with chondrogenic differentiation. Therefore, we termed these groups the 'chondrogenic surfaceome subset,' containing proteins such as collagens (COL2A1, COL6A1, COL9A2), TGFB2, and FGFR3.

We also performed a detailed PPI network analysis of each surfaceome cluster using STRING (Figure S4 in Supplementary file 1). In **Cluster 1**, the PPI network is enriched in ECM remodelling (MMP2, FN1, VCAN, DCN, PLOD1, CRTAP, P3H2, P4HA1/2), collagen biosynthesis (PLOD1, CRTAP, P3H2, P4HA1/2, P4HB), and protein folding (HSPA5/PDIA3), with additional roles in vesicle trafficking and oxidative stress response (PRDX6). The PPI network in **Cluster 2** was dominated by ephrin signalling with four Eph receptors (EPHB3, EPHA7, EPHB1, EPHB2), highlighting roles in developmental patterning. Endocytosis (AP2M1, RAB5C) and RAB GTPases (RAB5C, RAB14) are central to membrane dynamics and intracellular transport. SRC and FGFR2 link focal adhesion and growth factor signalling. **Cluster 3** is enriched in cytoskeletal organization (ACTN1, ACTN4, MYH9, ARF6), calcium signalling (CALM3, S100A6, ANXA1), and cell adhesion pathways (DMD, ARF6, RAP1B). Focal adhesion and actin cytoskeleton pathways dominate the network, driven by actinin, myosin, and dystrophin. Calcium signalling may integrate metabolic and inflammatory responses via CALM3 and S100A6. HMGB1 links nuclear DNA repair with extracellular VEGF signalling. **Cluster 4** is dominated by ephrin signalling with several Eph receptors (EPHA4, EPHA5, EPHB1, EPHB2, EPHB3, EPHA7), highlighting roles in cell migration during nodule formation. Wnt (FZD1/2/7) and Hedgehog (SMO) signalling pathways are central to developmental processes. EGFR/FGFRs (EGFR, FGFR2, FGFR3) link growth factor signalling to MAPK activation.

3. Surfaceome enrichment enhances detection of low-abundance targets

Comparative analysis revealed limited overlap (23%) between proteins identified in total lysates and surfaceome-enriched fractions (Table S2 in Supplementary file 1). Notably, 77% of AOB-enriched proteins were undetectable in total lysates, demonstrating the method's

enhanced capacity to resolve low-abundance membrane-associated targets. Conventional whole-cell proteomics is constrained by the dominance of high-abundance cytoplasmic and organellar proteins, which often mask low-abundance surface-residing targets during MS analysis. By selectively enriching surface proteins, our approach mitigates this dynamic range limitation, enabling robust identification of membrane-associated and extracellular proteins that otherwise fall below detection thresholds in unfractionated lysates. This methodological advance underscores the efficacy of this method in resolving biologically critical surfaceome components, which are frequently underrepresented in global proteomic analyses, and highlights its utility for advancing receptor, biomarker, and therapeutic target discovery.

4. In silico and in vitro chondrogenic surfaceome

To maximise the identification of cell surface proteins, we inferred cell surface localisation for all detected proteins using established GO annotations for cellular component and molecular function. We first applied this *in silico* prediction on the total cell lysate dataset, defining the GO term-based surfaceome of chondrogenic cultures. Of the 5,207 proteins in this dataset, 885 proteins (17%) were predicted to localis to the cell surface.

We then applied the same approach on the AOB-enriched dataset. The AOB-based enrichment method substantially increased the proportion of identified cell surface proteins, with 55–60% of proteins at all time points and across biological replicates annotated as cell surface-localised (Figure 6A). This represents a significant improvement in the number of surface proteins detected as chondrogenic differentiation progressed, as demonstrated by full symmetrical matrix analysis (Jaccard index) (Figure 6B). We classified the identified surfaceome proteins into major functional categories based on GO molecular function and biological process annotations: enzymes, transporters, receptors, cell junctions and adhesion proteins, ECM components, and unclassified/miscellaneous proteins (including known interacting or binding partners of surface proteins; Table 1). The relative distribution of surface proteins in these categories remained consistent throughout chondrogenesis.

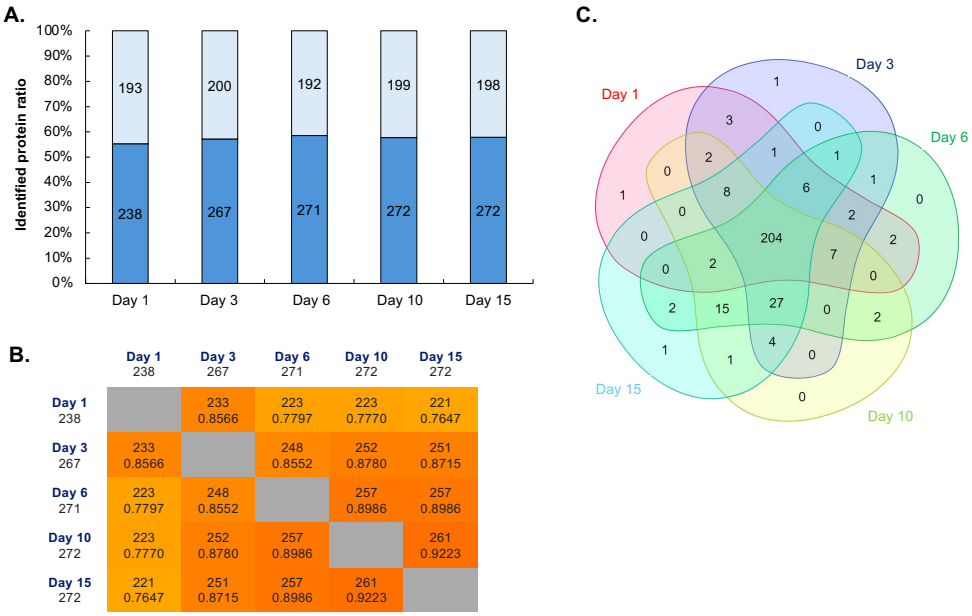

Figure 6. Enrichment of cell surface proteins using the AOB labelling approach. A. Distribution of the 504 surface proteins identified in this study (after manual curation using GO terms; dark bars, core surfaceome; light bars, probably non-surface proteins) between different culture days. **B.** Full symmetrical matrix of the surfaceome proteins across differentiating cultures (integers represent the number of surfaceome proteins; non-integers represent Jaccard indices). **C.** Distribution of the manually curated cell surface proteins identified in this study between micromass cultures of various ages.

We next examined qualitative expression dynamics of the cell surface proteins to identify candidate surface biomarkers specific to the early stages of chondrogenic differentiation (days 1–6). Using Venn diagram analysis of manually curated protein lists across the studied time points (Figure 6C), only two proteins met the criteria for early-stage specificity: ciliary neurotrophic factor receptor (CNTFR) and podocalyxin (PODXL).

	Day 1	Day 3	Day 6	Day 10	Day 15
Receptors	28%	29%	27%	28%	28%
Enzymes	33%	31%	32%	32%	31%
Transporters	21%	21%	19%	19%	20%
Adhesion proteins	24%	23%	23%	23%	23%
Miscellaneous	20%	24%	25%	25%	26%

Table 1. Relative distribution of GO functional classification of the identified surface proteins during chondrogenic differentiation in micromass cultures

5. Validation of ciliary neurotrophic factor receptor and podocalyxin expression in chondrogenic micromass cultures

To confirm the expression of CNTFR and PODXL in micromass cultures undergoing chondrogenesis, we performed western blot analysis on total cell lysates from micromass cultures harvested at the same time points as AOB-enriched samples. Both CNTFR and PODXL were detected on western blots. For CNTFR, a distinct band was observed at approximately 43 kDa, consistent with its predicted molecular mass, and its expression remained steady throughout the differentiation period (Figure 7A). Similarly, PODXL was detected as a prominent band at around 60 kDa with a steady expression pattern, although multiple bands were also present, which may reflect post-translational modifications (Figure 7B).

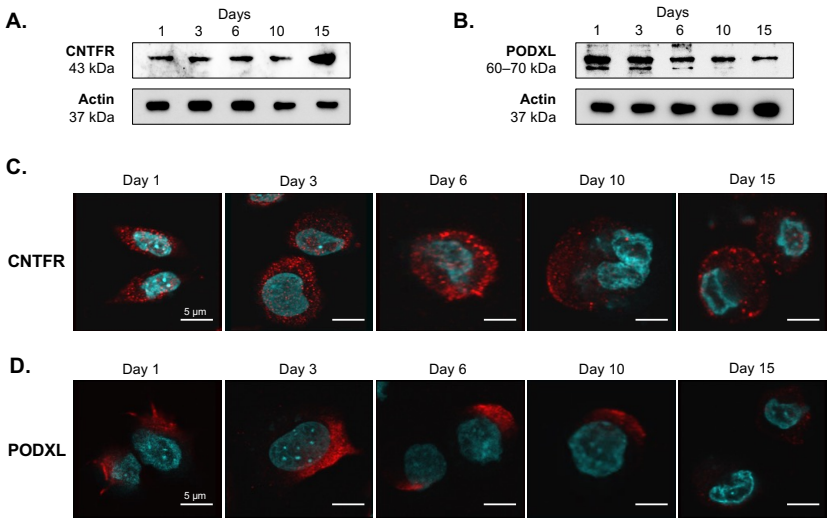

Figure 7. Validation of the efficacy and specificity of the AOB-based glycocapture method. Western blot for CNTFR (**A**) and PODXL (**B**) performed on total cell lysates of micromass cultures. Representative blot image (n=3). Full-length uncropped blots are presented in Fig. S5 in Supplementary file 1. Intracellular distribution of CNTFR (**C**) and PODXL (**D**) in cells of micromass cultures detected by immunocytochemistry. Primary antibodies were visualised using Alexa555-conjugated anti-rabbit secondary antibodies (red). Nuclear DNA was stained with DAPI (cyan). Data shown are representative out of 3 independent experiments. Scale bar, 5 µm.

To further investigate the subcellular localization of CNTFR and PODXL, we carried out immunocytochemistry followed by confocal microscopy. Both CNTFR and PODXL were localised to the plasma membrane in chondrogenic cells, with additional intracellular staining (Figure 7C–D). Although this analysis was qualitative, both markers appeared to be

downregulated at later stages of differentiation, with this trend being particularly pronounced for PODXL. Notably, PODXL was primarily localised at the leading edge of cellular processes, suggesting a potential role in cell morphology or migration during chondrogenesis (Figure 7D).

To investigate the functional role of CNTFR and PODXL in our chondrogenic model, we analysed their regulatory networks using transcriptomic and proteomic data. STRING-derived interaction network for both proteins (top 25 interactants) were cross-referenced with expression profiles from our previously published RNA-seq dataset (Takacs et al., 2023b) of the same chondrogenic model, and total lysate proteomics.

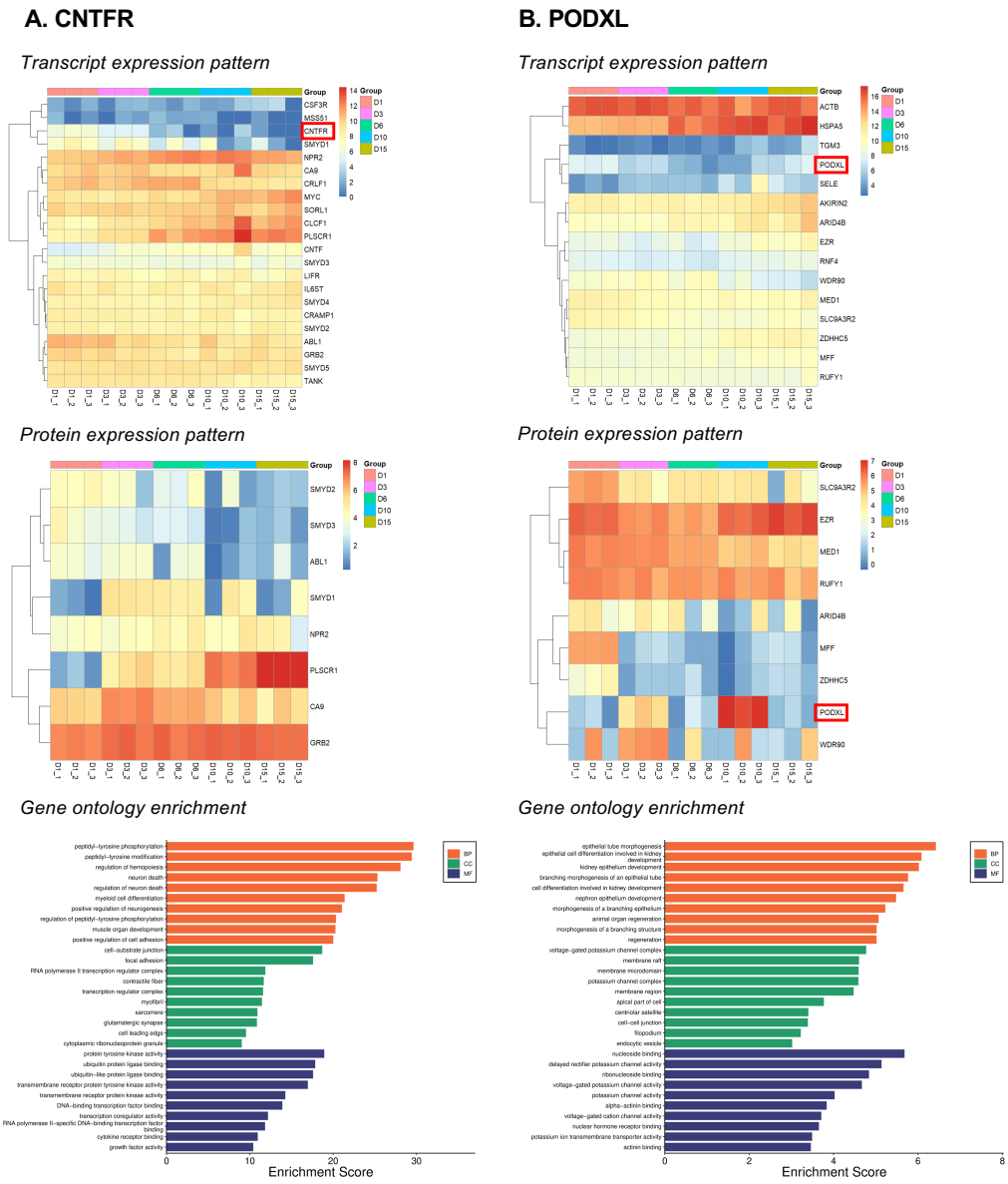

Figure 8. Transcript and protein expression patterns for the closest 25 interactants, as well as WGCNA co-expression networks, and enriched gene ontology (GO) terms in the MEs for CNTFR (**A**) and PODXL (**B**).

For CNTFR, 21 of the 25 interactants were expressed at the transcript level (Figure 8A), and 8 also detected as proteins in the total lysates. PODXL showed expression of 14 interactant transcripts (Figure 8B) and 8 corresponding proteins. Weighted gene co-expression network analysis (WGCNA) of RNA-seq data, using CNTFR or PODXL expression levels across different samples as a trait, revealed clusters of genes highly correlated with CNTFR or PODXL expression (Figure S6 in Supplementary file 1). Therefore, we screened the proximal associated proteins of CNTFR or PODXL and their top 25 interactants within significantly correlated modules and integrated them. The rationale behind this approach was to check the enrichment of GO information in the co-expression modules. For CNTFR, five module eigengenes (MEs) were showing significant degree of correlation (with the turquoise module showing the strongest correlation to the trait), indicating that genes in these MEs may be associated with CNTFR or its top 25 interactants. We therefore performed functional enrichment analysis on these modules, in which GO terms related to tyrosine phosphorylation, cell adhesion, cytokine and growth factor activity were significantly enriched, in addition to the PI3K–Akt and MAPK signalling pathways. For PODXL, out of five MEs showing high degree of correlation with the gene and its interactants, the black ME displayed the strongest correlation to the trait, in which GO terms such as cell-cell junction, potassium channel activity, alongside terms related to differentiation and morphogenesis were significantly over-represented.

6. Transient gene silencing of CNTFR and PODXL

To assess the roles of CNTFR and PODXL in chondrogenesis, we transiently silenced their expression in chondrogenic progenitor cells using siRNA delivered via Lipofectamin prior to seeding as micromass cultures (day 0). Transfection efficacy was confirmed in 2-day-old cultures (48 hours post-silencing), with CNTFR and PODXL mRNA levels reduced to 57% and 49%, respectively, compared to NT controls (Figure 9A). Silencing neiter CNTFR nor PODXL influenced cartilage ECM deposition by day 6, as revealed by unchanged metachromatic staining intensity and subsequent image analysis (Figure 9B), nor did it affect the rate of cell

proliferation by day 6 measured by MTT assays (Figure 9C). However, RT-qPCR analysis of key osteochondrogenic marker genes 2 days post-transfection revealed distinct transcriptional effects (Figure 9D). Transient silencing of CNTFR led to a significant upregulation of ACAN, COL1A1, COL2A1, and RUNX2 expression (2.9-, 2.7-, 4.9-, and 2.5-fold *versus* NT control, respectively). In contrast, while PODXL silencing significantly increased ACAN and RUNX2 expression (3.3- and 2.6-fold, respectively), it resulted in a marked downregulation of COL1A1 (–3.8-fold), indicating divergent regulatory roles in ECM gene expression.

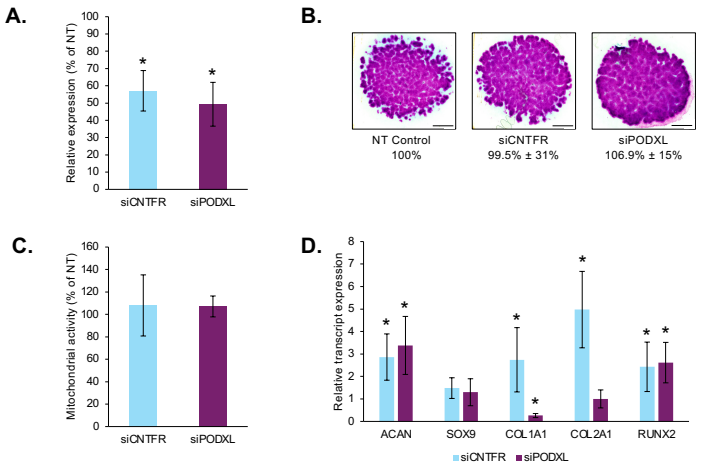

Figure 9. Effects of transient gene silencing of CNTFR or PODXL in chondrogenic cultures on chondrogenesis and osteochondral marker gene expression profiles. A. Gene expression data of CNTFR or PODXL following transient gene silencing 48 hours post transfection. Relative gene expression values are calculated by normalising to RPS7. Data are expressed as mean ± SEM (N=3). Significant differences ($p < 0.05$) in relative gene expression data relative to non-targeting (NT) controls are indicated by an asterisk (*). **B.** Metachromatic cartilage areas after DMMB staining of 6-day-old micromass cultures following transfection with CNTFR, PODXL siRNA, or NT control. Original magnification was ×4. Scale bar, 1 mm. Values are results of a MATLAB-based image analysis of metachromatic areas. Data are expressed as mean ± SEM, compared to NT (100%). Representative data of 3 biological replicates. **C.** MTT assay results carried out 6 days post electroporation with siCNTFR or siPODXL, normalised to the NT control. Average data of 3 biological replicates. **D.** Gene expression data of selected osteo/chondrogenic markers 48 hours after transient gene silencing. Relative gene expression values are calculated by normalising to RPS7. Data are expressed as mean ± SEM (N=3). Significant differences ($p < 0.05$) in relative gene expression data relative to NT controls are indicated by an asterisk (*).

Although neither perturbation affected observable changes in ECM deposition or proliferation, these findings highlight distinct effects on transcriptional regulation of ECM-associated genes by CNTFR and PODXL. The contrasting modulation of COL1A1, in particular, suggests that these surface proteins may influence not only the quantity but also the qualitative composition and molecular specificity of the ECM during chondrogenesis.

Discussion

To our knowledge, this study provides the first comprehensive quantitative analysis of the surfaceome of chondrogenic cells in an established *in vitro* model, identifying podocalyxin (PODXL) and ciliary neurotrophic factor receptor (CNTFR) as novel components. Our glycocapture-assisted enrichment approach, coupled with high-throughput shotgun mass spectrometry, offering distinct advantages over traditional surfaceome profiling methods (Pauwels et al., 2022; Kovacs et al., 2025). By targeting sialic acid residues on surface glycoproteins, this strategy achieves superior selectivity and may outperform several existing proteomic methods such as lectin-based affinity capture or hydrophilic chromatography separation (Lee and Sun, 2014), enabling robust identification of low-abundance membrane proteins often obscured in whole-cell proteomics.

The discovery of CNTFR and PODXL within the chondrogenic surfaceome may offer new insights into understanding the molecular mechanisms of chondrogenesis, with potential implications for cartilage disorders such as OA. Ciliary neurotrophic factor (CNTF) is a cytokine that belongs to the interleukin-6 (IL-6) family. It signals through a receptor complex consisting of CNTF receptor α (CNTFR), gp130 (encoded by the IL6ST gene), and leukaemia inhibitory factor receptor (LIFR) (Sleeman et al., 2000; Pasquin et al., 2015). CNTF was initially identified as a growth factor that stimulates gene expression, survival or differentiation of neurons, but has since been shown to have pleiotropic effects in various tissues, including bone and cartilage (McGregor et al., 2010; Crisponi et al., 2022). In female mice, CNTF acts as an inhibitor of trabecular bone formation, while in male mice, it stimulates cortical growth (McGregor et al., 2010). This sexual dimorphism in the effects of CNTF effects suggests that CNTF may have complex, context-dependent functions in the bone marrow microenvironment (Askmyr et al., 2015). Notably, cardiotrophin-like cytokine (CLCF1), a neurotrophic factor and a ligand of CNTFR, influences MSC differentiation and osteogenesis *in vitro* (Nahle et al., 2019), suggesting broader roles for this cytokine in skeletal development.

In chondrocytes and osteoblast-like cells, the CNTFR axis plays significant roles (Tsuritani et al., 2010). CNTF/CNTFR signalling has been implicated in cartilage homeostasis

and osteoarthritis (OA) progression. Upregulation of the CRLF1/CLCF1 complex, which competes with CNTF for CNTFR binding, disrupts cartilage homeostasis and exacerbates OA progression by dysregulating chondrocyte proliferation and ECM synthesis (Crisponi et al., 2022). Our finding of persistent CNTFR expression during chondrogenesis aligns with its dual role in maintaining cartilage integrity and mediating pathological remodelling, positioning it as a potential therapeutic node in OA.

One of the more intriguing findings from our transient knockdown experiments was the opposing regulation of COL1A1 following PODXL versus CNTFR silencing. While CNTFR knockdown upregulated COL1A1 (2.7-fold), a well-known marker of fibrocartilage and mechanically compromised repair tissue (Dehne et al., 2010; Embree et al., 2016), PODXL silencing reduced its expression substantially (−3.8-fold). This dichotomy suggests distinct roles for these surface proteins in regulating ECM composition. PODXL may promote fibrogenic signalling via β1-integrin/FAK pathways, potentially maintaining progenitor states that favour type I collagen deposition (Khurana et al., 2016; Jiang et al., 2024). Conversely, CNTFR loss might mimic cytokine deprivation stress, activating compensatory fibrotic programmes reminiscent of synovial fibrosis in OA via impaired signalling (Damerau et al., 2024).

Notably, these transcriptional changes occurred in the absence of detectable changes in ECM production or proliferation (Figure 9B–C), suggesting either functional redundancy in matrix remodelling or post-transcriptional buffering. Given that PODXL expression is minimal in human OA cartilage (Figure S7 in Supplementary file 1), the relevance of this regulatory axis in disease contexts remains to be clarified, further underscoring the need for validation in adult or disease-specific models. Future studies might explore whether PODXL or CNTFR modulate ERK/STAT3 cross-talk to influence collagen isoform switching during chondrogenesis.

Nevertheless, to our knowledge, this is the first study to demonstrate plasma membrane localization of CNTFR in differentiating chondrocytes. This finding expands the potential roles of neurotrophic signalling in primary cartilage development, as CNTFR and

most of its known interactants were expressed at both mRNA and protein levels. In OA, where altered signalling pathways contribute to disease progression, CNTFR could represent a novel therapeutic target (Tsuritani et al., 2010). However, mechanistic studies are required to elucidate how CNTF and its receptor complex regulate chondrocyte differentiation and homeostasis, particularly in injury or degenerative contexts.

Podocalyxin (PODXL), a member of the CD34 family of transmembrane sialomucins, is classically associated with kidney podocytes and vascular endothelium (Le Tran et al., 2021). Its established roles in cell adhesion, migration, and differentiation in various cell types (Lee et al., 2009) make its detection in chondrogenic cells a novel observation with implications for skeletal biology. In MSCs and skeletal development, PODXL is a marker of early progenitor populations with enhanced differentiation potential. High PODXL expression, often co-occurring with α6-integrin (CD49f), characterizes low-density MSC cultures exhibiting superior clonogenicity and osteochondrogenic capacity (Lee et al., 2009). Notably, PODXL downregulation during osteogenic maturation suggests a role in maintaining progenitor states rather than supporting terminally differentiated functions (Lee et al., 2009).

While direct evidence linking PODXL to chondrocyte differentiation and function remains limited, its role in MSC and osteogenic differentiation, as well as cell adhesion and migration (Larrucea et al., 2008) aligns with processes critical to cartilage morphogenesis. Chondrogenesis is regulated by various factors, including the master transcription factor SOX9 and growth factors such as TGF-β (Chen et al., 2021). The expression of PODXL in early progenitor cells may modulate their responsiveness to these chondrogenic signals. The co-expression of numerous PODXL interactants in our model underscores its potential involvement, but mechanistic research is needed to define the specific molecular mechanisms by which PODXL influences chondrogenesis.

Further studies into these pathways could inform regenerative medicine strategies targeting cartilage disorders (Peng et al., 2023). However, the functional role of PODXL in chondrogenesis remains to be fully elucidated, and additional validation, particularly in human models, is necessary to confirm its relevance.

The identification of these novel surface proteins on chondrogenic cells may provide valuable new biomarkers for early OA detection and disease monitoring, addressing a critical unmet need in the field (Mobasheri et al., 2023). Their expression on chondrogenic cells could enable the earlier identification of cartilage changes, potentially before irreversible damage occurs. Notably, transcripts for both CNTFR and PODXL were detected in single-cell RNA-seq analyses of human articular chondrocyte subpopulations (Figure S7 in Supplementary file 1). While CNTFR expression was predominant in effector and homeostatic chondrocytes (EC and HomC), PODXL transcripts were present at much lower levels, particularly in VEGFA^{+} cells, fibrochondrocytes, and pre-hypertrophic chondrocytes.

Alterations in PODXL or CNTFR levels could potentially be detected in synovial fluid or serum prior to the onset of clinical symptoms (Henrotin, 2022). This could lead to the development of minimally invasive diagnostic tests for early-stage OA. Monitoring changes in PODXL and CNTFR levels may also provide insight into disease progression, enabling more timely and targeted interventions. Furthermore, these markers could serve as useful indicators for evaluating therapeutic responses, as their expression levels might reflect treatment efficacy. Incorporating PODXL and CNTFR into existing biomarker panels could improve diagnostic and prognostic accuracy. Combining these novel markers with established ones such as CTX-II, COMP, or MMPs may offer a more comprehensive assessment of disease status and progression (Mobasheri et al., 2023), ultimately supporting more personalized treatment strategies based on individual biomarker profiles.

Beyond their diagnostic potential, these proteins represent promising targets therapeutic in OA-related contexts. For example, modulating PODXL-mediated cell-matrix interactions or CNTFR signalling pathways may offer new approaches to cartilage repair or OA management. Harnessing CNTFR-mediated signalling could enhance the effectiveness of growth factor-based therapies in cartilage regeneration (Zhang et al., 2024). Although silencing of CNTFR and PODXL did not yield overt changes in ECM deposition or cell proliferation in our model, this does not rule out their involvement in key regulatory pathways during chondrogenesis. Functional redundancy within the chondrogenic signalling network or

compensatory mechanisms from other surface receptors may have masked the phenotypic impact of individual gene knockdowns. Clarifying their roles may require combinatorial gene silencing approaches, time-resolved transcriptomics, or integrative pathway-level analysis.

Limitations and conclusions

While this study advances our understanding of the chondrogenic surfaceome, it is important to acknowledge its limitations. The use of chicken embryonic limb bud-derived chondrogenic progenitor cells, while offering advantages for developmental studies, may not fully recapitulate human chondrogenesis. Similarly, the micromass culture system, while well-validated, simplifies the *in vivo* complexity of articular cartilage development. Nevertheless, the chicken model remains instrumental for elucidating fundamental principles of vertebrate cartilage development and offers unique advantages for studying embryonic processes (Takacs et al., 2023a). Additionally, our cell surface protein enrichment method primarily captures N-linked glycoproteins, potentially overlooking other (non-glycosylated or O-linked) surface targets.

We applied human Gene Ontology (GO) terms to proteomics data obtained on the chicken model, justified by the fact that Gene Ontology is designed to be largely species-neutral, making it well-suited for cross-species use (Primmer et al., 2013). This allows functional annotations derived from model organisms, such as humans, to be transferred to inferred orthologues in other species, including chickens (Primmer et al., 2013). Chickens and humans share a significant number of orthologous genes. About 60 percent of chicken genes correspond to a similar human gene (Wallis et al., 2004). This high degree of conservation, especially in genes involved in basic cellular functions, provides a foundation for using human GO terms in chicken studies. Moreover, while human GO annotations are more comprehensively curated compared to those of many other species, including chickens. Our study aims to understand biological processes that are relevant to human health or comparative biology (Wallis et al., 2004). However, it is important to highlight that some

biological processes may be unique to birds or chickens, which might not be adequately represented in human GO terms (Wallis et al., 2004).

Despite these constraints, our work offers several notable advantages. The chicken micromass model offers unique advantages for studying early developmental processes, bridging developmental biology and OA research. Our glycocapture-mass spectrometry pipeline allows for a more complete characterization of the chondrogenic cell surfaceome compared to conventional antibody-based methods, which are limited by antibody availability (Gundry et al., 2008). The use of high-throughput shotgun mass spectrometry enables systematic, quantitative surfaceome profiling across different stages of chondrogenesis, offering a platform for future mechanistic exploration.

In conclusion, this study maps the chondrogenic surfaceome and identifies PODXL and CNTFR as novel candidates with potential relevance to OA. While further validation in human preclinical models is essential, these findings open new avenues for biomarker discovery and therapeutic targeting in cartilage disorders.

AUTHOR CONTRIBUTIONS

All authors made substantial contributions to discussion of the content, writing of the original outline, and reviewing/editing of the article before submission. All authors approve the final version for publication and agree to be accountable for the accuracy and integrity of the study.

Patrik Kovács: Formal analysis, Methodology, Validation, Visualisation, Writing—original draft, Writing—review & editing. Péter Brázda: Formal analysis, Visualisation, Writing—original draft, Writing—review & editing. Tibor Hajdú: Formal analysis, Methodology, Writing—original draft, Writing—review & editing. Boglárka Harsányi: Formal analysis, Methodology, Writing—original draft. Krisztián Juhász: Formal analysis, Methodology, Writing—original draft. Roland Takács: Formal analysis, Methodology, Validation, Writing—original draft, Writing—review & editing. Judit Vágó: Formal analysis, Methodology, Writing—original draft, Writing—review &

editing. Zhangzgeng Wang: Formal analysis, Methodology, Writing—original draft, Writing—review & editing. Clare Coveney: Formal analysis, Methodology, Writing—original draft, Writing—review & editing. David J. Boocock: Formal analysis, Software, Methodology, Visualization, Writing—original draft, Writing—review & editing. Csaba Matta: Conceptualization, Formal analysis, Funding acquisition, Methodology, Supervision, Validation, Writing—original draft, Writing—review & editing.

ACKNOWLEDGEMENTS

The authors thank Mrs. Krisztina Biróné Barna and Ms. Éva Katona from the Department of Anatomy, Histology and Embryology, and Prof. Éva Csősz and Mrs. Julianna Kökényesiné Csáki from the Proteomics Core Facility, Department of Biochemistry and Molecular Biology, Faculty of Medicine, University of Debrecen, for technical assistance.

FUNDING

This paper was supported by the János Bolyai Research Scholarship of the Hungarian Academy of Sciences, awarded to CM. CM was supported by the Young Researcher Excellence Programme (grant number: FK-134304) of the National Research, Development and Innovation Office, Hungary. This research was supported by the EKÖP-24-4 and EKÖP-24-3 University Research Fellowship Programme of the Ministry for Culture and Innovation from the source of the National Research, Development and Innovation Fund, Hungary, awarded to RT (EKÖP-24-4-II-DE-58), KJ (EKÖP-24-3-I-DE-290) and PK (EKÖP-24-3-II-DE-1). PK was supported by the PhD Excellence Scholarship from the Count István Tisza Foundation for the University of Debrecen. CM and RT also acknowledge financial support from the European Cooperation in Science and Technology COST Association Action CA21110 - Building an open European Network on OsteoArthritis research (NetwOArk); https://www.cost.eu/actions/CA21110/). This research was supported by the University of Debrecen Program for Scientific Publication.

CONFLICT OF INTEREST

The authors declare that they have no conflicts of interest. The authors wrote this paper within the scope of their academic and research positions. None of the authors has any relationships that could be construed as biased or inappropriate. Funding bodies were not involved in the study design, data collection, analysis, or interpretation. The decision to submit this paper for publication was not influenced by any funding bodies.

References

1. Alegre-Aguaron, E., Desportes, P., Garcia-Alvarez, F., Castiella, T., Larrad, L., and Martinez-Lorenzo, M.J. (2012). Differences in surface marker expression and chondrogenic potential among various tissue-derived mesenchymal cells from elderly patients with osteoarthritis. Cells Tissues Organs 196, 231-240.
2. Askmyr, M., White, K.E., Jovic, T., King, H.A., Quach, J.M., Maluenda, A.C., Baker, E.K., Smeets, M.F., Walkley, C.R., and Purton, L.E. (2015). Ciliary neurotrophic factor has intrinsic and extrinsic roles in regulating B cell differentiation and bone structure. Sci Rep 5, 15529.
3. Bayliss, L.E., Culliford, D., Monk, A.P., Glyn-Jones, S., Prieto-Alhambra, D., Judge, A., Cooper, C., Carr, A.J., Arden, N.K., Beard, D.J.*, et al.* (2017). The effect of patient age at intervention on risk of implant revision after total replacement of the hip or knee: a population-based cohort study. Lancet 389, 1424-1430.
4. Chen, H., Tan, X.N., Hu, S., Liu, R.Q., Peng, L.H., Li, Y.M., and Wu, P. (2021). Molecular Mechanisms of Chondrocyte Proliferation and Differentiation. Front Cell Dev Biol 9, 664168.
5. Crisponi, L., Buers, I., and Rutsch, F. (2022). CRLF1 and CLCF1 in Development, Health and Disease. Int J Mol Sci 23.
6. Damerau, A., Rosenow, E., Alkhoury, D., Buttgereit, F., and Gaber, T. (2024). Fibrotic pathways and fibroblast-like synoviocyte phenotypes in osteoarthritis. Front Immunol 15, 1385006.
7. Dehne, T., Schenk, R., Perka, C., Morawietz, L., Pruss, A., Sittinger, M., Kaps, C., and Ringe, J. (2010). Gene expression profiling of primary human articular chondrocytes in high-density micromasses reveals patterns of recovery, maintenance, re- and dedifferentiation. Gene 462, 8-17.
8. Demichev, V., Messner, C.B., Vernardis, S.I., Lilley, K.S., and Ralser, M. (2020). DIA-NN: neural networks and interference correction enable deep proteome coverage in high throughput. Nat Methods 17, 41-44.
9. Embree, M.C., Chen, M., Pylawka, S., Kong, D., Iwaoka, G.M., Kalajzic, I., Yao, H., Shi, C., Sun, D., Sheu, T.J.*, et al.* (2016). Exploiting endogenous fibrocartilage stem cells to regenerate cartilage and repair joint injury. Nat Commun 7, 13073.
10. Gundry, R.L., Boheler, K.R., Van Eyk, J.E., and Wollscheid, B. (2008). A novel role for proteomics in the discovery of cell-surface markers on stem cells: Scratching the surface. Proteomics Clin Appl 2, 892-903.
11. Henrotin, Y. (2022). Osteoarthritis in year 2021: biochemical markers. Osteoarthritis Cartilage 30, 237-248.
12. Im, G.I., and Kim, T.K. (2020). Regenerative Therapy for Osteoarthritis: A Perspective. Int J Stem Cells 13, 177-181.
13. Jeremiasse, B., Matta, C., Fellows, C.R., Boocock, D.J., Smith, J.R., Liddell, S., Lafeber, F., van Spil, W.E., and Mobasheri, A. (2020). Alterations in the chondrocyte surfaceome in response to pro-inflammatory cytokines. BMC Mol Cell Biol 21, 47.

14. Jiang, C., Centonze, A., Song, Y., Chrisnandy, A., Tika, E., Rezakhani, S., Zahedi, Z., Bouvencourt, G., Dubois, C., Van Keymeulen, A.*, et al.* (2024). Collagen signaling and matrix stiffness regulate multipotency in glandular epithelial stem cells in mice. Nat Commun 15, 10482.
15. Kalamegam, G., Memic, A., Budd, E., Abbas, M., and Mobasheri, A. (2018). A Comprehensive Review of Stem Cells for Cartilage Regeneration in Osteoarthritis. Adv Exp Med Biol 1089, 23-36.
16. Khurana, S., Schouteden, S., Manesia, J.K., Santamaria-Martinez, A., Huelsken, J., Lacy-Hulbert, A., and Verfaillie, C.M. (2016). Outside-in integrin signalling regulates haematopoietic stem cell function via Periostin-Itgav axis. Nat Commun 7, 13500.
17. Kovacs, P., Boocock, D.J., Coveney, C., Mobasheri, A., and Matta, C. (2025). Aminooxy Biotin-Based Characterization of the Surfaceome of Chondrogenic Cells. Methods Mol Biol 2908, 65-79.
18. Larrucea, S., Butta, N., Arias-Salgado, E.G., Alonso-Martin, S., Ayuso, M.S., and Parrilla, R. (2008). Expression of podocalyxin enhances the adherence, migration, and intercellular communication of cells. Exp Cell Res 314, 2004-2015.
19. Le Tran, N., Wang, Y., and Nie, G. (2021). Podocalyxin in Normal Tissue and Epithelial Cancer. Cancers (Basel) 13.
20. Lee, M.C., and Sun, B. (2014). Glycopeptide capture for cell surface proteomics. J Vis Exp.
21. Lee, R.H., Seo, M.J., Pulin, A.A., Gregory, C.A., Ylostalo, J., and Prockop, D.J. (2009). The CD34-like protein PODXL and alpha6-integrin (CD49f) identify early progenitor MSCs with increased clonogenicity and migration to infarcted heart in mice. Blood 113, 816-826.
22. Lu, Z., Yan, L., and Pei, M. (2020). Commentary on 'Surface markers associated with chondrogenic potential of human mesenchymal stromal/stem cells'. F1000Res 9.
23. Maqbool, M., Fekadu, G., Jiang, X., Bekele, F., Tolossa, T., Turi, E., Fetensa, G., and Fanta, K. (2021). An up to date on clinical prospects and management of osteoarthritis. Ann Med Surg (Lond) 72, 103077.
24. Matta, C., Boocock, D.J., Fellows, C.R., Miosge, N., Dixon, J.E., Liddell, S., Smith, J., and Mobasheri, A. (2019a). Molecular phenotyping of the surfaceome of migratory chondroprogenitors and mesenchymal stem cells using biotinylation, glycocapture and quantitative LC-MS/MS proteomic analysis. Sci Rep 9, 9018.
25. Matta, C., Juhasz, T., Fodor, J., Hajdu, T., Katona, E., Szucs-Somogyi, C., Takacs, R., Vago, J., Olah, T., Bartok, A.*, et al.* (2019b). N-methyl-D-aspartate (NMDA) receptor expression and function is required for early chondrogenesis. Cell Commun Signal 17, 166.
26. McGregor, N.E., Poulton, I.J., Walker, E.C., Pompolo, S., Quinn, J.M., Martin, T.J., and Sims, N.A. (2010). Ciliary neurotrophic factor inhibits bone formation and plays a sex-specific role in bone growth and remodeling. Calcif Tissue Int 86, 261-270.
27. Mobasheri, A., Thudium, C.S., Bay-Jensen, A.C., Maleitzke, T., Geissler, S., Duda, G.N., and Winkler, T. (2023). Biomarkers for osteoarthritis: Current status and future prospects. Best Pract Res Clin Rheumatol 37, 101852.
28. Muthu, S., Korpershoek, J.V., Novais, E.J., Tawy, G.F., Hollander, A.P., and Martin, I. (2023). Failure of cartilage regeneration: emerging hypotheses and related therapeutic strategies. Nat Rev Rheumatol 19, 403-416.
29. Nahle, S., Pasquin, S., Laplante, V., Rousseau, F., Sharma, M., and Gauchat, J.F. (2019). Cardiotrophin-like cytokine (CLCF1) modulates mesenchymal stem cell osteoblastic differentiation. J Biol Chem 294, 11952-11959.
30. Pasquin, S., Sharma, M., and Gauchat, J.F. (2015). Ciliary neurotrophic factor (CNTF): New facets of an old molecule for treating neurodegenerative and metabolic syndrome pathologies. Cytokine Growth Factor Rev 26, 507-515.
31. Pauwels, J., Fijalkowska, D., Eyckerman, S., and Gevaert, K. (2022). Mass spectrometry and the cellular surfaceome. Mass Spectrom Rev 41, 804-841.
32. Peng, Y., Jiang, H., and Zuo, H.D. (2023). Factors affecting osteogenesis and chondrogenic differentiation of mesenchymal stem cells in osteoarthritis. World J Stem Cells 15, 548-560.

33. Pfaffl, M.W., Tichopad, A., Prgomet, C., and Neuvians, T.P. (2004). Determination of stable housekeeping genes, differentially regulated target genes and sample integrity: BestKeeper--Excel-based tool using pair-wise correlations. Biotechnol Lett 26, 509-515.
34. Primmer, C.R., Papakostas, S., Leder, E.H., Davis, M.J., and Ragan, M.A. (2013). Annotated genes and nonannotated genomes: cross-species use of Gene Ontology in ecology and evolution research. Mol Ecol 22, 3216-3241.
35. Ranathunge, C., Patel, S.S., Pinky, L., Correll, V.L., Chen, S., Semmes, O.J., Armstrong, R.K., Combs, C.D., and Nyalwidhe, J.O. (2023). promor: a comprehensive R package for label-free proteomics data analysis and predictive modeling. Bioinform Adv 3, vbad025.
36. Richardson, S.M., Kalamegam, G., Pushparaj, P.N., Matta, C., Memic, A., Khademhosseini, A., Mobasheri, R., Poletti, F.L., Hoyland, J.A., and Mobasheri, A. (2016). Mesenchymal stem cells in regenerative medicine: Focus on articular cartilage and intervertebral disc regeneration. Methods 99, 69-80.
37. Rodriguez-Merchan, E.C. (2023). The Current Role of Disease-modifying Osteoarthritis Drugs. Arch Bone Jt Surg 11, 11-22.
38. Sleeman, M.W., Anderson, K.D., Lambert, P.D., Yancopoulos, G.D., and Wiegand, S.J. (2000). The ciliary neurotrophic factor and its receptor, CNTFR alpha. Pharm Acta Helv 74, 265-272.
39. Takacs, R., Juhasz, T., Katona, E., Somogyi, C., Vago, J., Hajdu, T., Barna, K.B., Nagy, P., Zakany, R., and Matta, C. (2023a). Isolation and Micromass Culturing of Primary Chicken Chondroprogenitor Cells for Cartilage Regeneration. Curr Protoc 3, e835.
40. Takacs, R., Mobasheri, A., and Matta, C. (2025). Introduction: Methods for Studying the Plasma Membrane and the Surfaceome. Methods Mol Biol 2908, 1-9.
41. Takacs, R., Vago, J., Poliska, S., Pushparaj, P.N., Ducza, L., Kovacs, P., Jin, E.J., Barrett-Jolley, R., Zakany, R., and Matta, C. (2023b). The temporal transcriptomic signature of cartilage formation. Nucleic Acids Res 51, 3590-3617.
42. Tong, L., Yu, H., Huang, X., Shen, J., Xiao, G., Chen, L., Wang, H., Xing, L., and Chen, D. (2022). Current understanding of osteoarthritis pathogenesis and relevant new approaches. Bone Res 10, 60.
43. Tsuritani, K., Takeda, J., Sakagami, J., Ishii, A., Eriksson, T., Hara, T., Ishibashi, H., Koshihara, Y., Yamada, K., and Yoneda, Y. (2010). Cytokine receptor-like factor 1 is highly expressed in damaged human knee osteoarthritic cartilage and involved in osteoarthritis downstream of TGF-beta. Calcif Tissue Int 86, 47-57.
44. Wallis, J.W., Aerts, J., Groenen, M.A., Crooijmans, R.P., Layman, D., Graves, T.A., Scheer, D.E., Kremitzki, C., Fedele, M.J., Mudd, N.K*., et al.* (2004). A physical map of the chicken genome. Nature 432, 761-764.
45. Zhang, F., Clair, A.J., Dankert, J.F., Lee, Y.J., Campbell, K.A., and Kirsch, T. (2024). Cytokine Receptor-like Factor 1 (CRLF1) and Its Role in Osteochondral Repair. Cells 13.